A Novel Aspect on Structural Formation of Physical Gels

Che-Min Chou and Po-Da Hong*

Department of Polymer Engineering, National Taiwan University of Science and Technology, Taipei, 10607, Taiwan

Received November 14, 2002; Revised Manuscript Received July 11, 2003

ABSTRACT: By using the time-resolved small angle light scattering (TRSALS) technique, we present the first real-time measurement of the physical gelation process for a crystalline polymer. The finding is that the light scattering patterns show a unique feature in the H_v and the V_v scattering for PVDF gel electrolytes. More significant is the fact that the initial H_v scattering pattern with a four-leaf-clover shape gradually turns into a final pattern with 2-fold structure, composed of an X-type and a four-crescent-moon shape at low and high q ranges, respectively. The experimental results are noteworthy in that they show the characteristics of the special birefingent transition, i.e., the anisotropic-to-isotropic transition in the gelation process. Our observations illustrate a novel aspect in the structural formation of physical gels. During the course of the gelation we observed the existence of three distinct time regimes: (i) a nucleation and growth stage, where the droplet formation can be interpreted in terms of the simultaneous formation of crystallites or fibril texture with the growth of the birefringent droplets and the crystallites or the fibrils act as junction points in the droplets, leading to approximate dispersion of the hard spheres in the solutions; (ii) the dynamic cluster-to-percolation transition stage, where the large-scale concentration fluctuation is triggered by the hard spheres diffusion and aggregation to form the macroscopic percolation structures and where this main characteristics of the process is simultaneously accompanied by the anisotropic-to-isotropic transition; (iii) a ripening process in the late stage of gelation that causes the arrangement and growth of microstructures such as crystallites or fibrils to be highly concentrated. It is clear that these experimental results are entirely different from previous understandings of spinodal gels. We may proceed from these results to conclude that the formation of the birefringent droplets and the colloid aggregation dominate the physical gelation process in the present work.

Introduction

Gelation is the phase transition from a collection of finite clusters to a state with the formation of an infinite network. The essential physical feature of a gel is its geometrical connections, and hence theoretical progress generally emphasizes percolation phenomena to gelation theory.[1,2] In addition to this, an even more noteworthy subject is the nature and formation of network junctions in physical gels. A thermoreversible physical gel is a three-dimensional network of polymer chains cross-linked by physical junctions, and it can arise either as the result of a phase transition or through some specific molecular association or as a result of entanglements.[3] In the present study, we confine our attention to the case of gels associated with phase transition. Physical gels passing through phase transition are especially complex systems, and it is generally accepted that the gelation is typically governed by the coupling of several phase transitions like the liquid−liquid-phase separation,[4,5] the crystallite formation of the polymer chain segments,[6,7] and percolation phenomena. However, the complexity introduced by these coupling mechanisms has limited theoretical progress largely to purely phenomenological approaches, resulting in difficulties to explain fully in terms of gelation phenomena.

Most studies of gelation behaviors have focused on phase behavior and structural morphology in physical gels.[8−11] Experimentally, there is a lack of data on the dynamics of the gelation process, which may be attributed to both the complex nature of the gelation phenomena and practical difficulties in real-time observation of structural development of physical gels. Our previous papers considered, from the thermodynamic and kinetic points of view, the essential effects on gelation of crystallization and phase separation, then proposing a schematic model for the hierarchic structure of physical gels.[12,13] However, in our previous papers there were no real-time observations for structural evolution during the physical gelation.

Small-angle light scattering is one of the most useful techniques to study mesoscopic disordered systems that present inhomogeneities on length scales at the order of the wavelength of light, or larger. Examples can be found in the fields of colloidal aggregation,[14,15] polymer blends,[16,17] gel formation,[18,19] and, in general, the chemical physics of complex fluids and critical phenomena. To perform real-time measurements of the gelation process, we designed a time-resolved small-angle light scattering (TRSALS) apparatus with the pixel array of a superb dynamic range (16-bit) charge coupled device (CCD) camera, allowing us to perform azimuthal averages of the structural function in the case of isotropic scattering, or to detect the optical anisotropy scattering in an oriented system. By using the TRSALS technique, we present the first real-time measurement of crystal nucleation and concentration fluctuation during the gelation process of a polymer solution and observed results which illustrate a novel aspect in the structural formation of physical gels.

Experimental Sections

Materials. The crystalline polymer used in this study is poly(vinylidene fluoride) (PVDF) powder ($M_w = 2.75 \times 10^5$ and $M_w/M_n = 2.57$, Aldrich Chem. Co.). The solvent was mixture of tetra(ethylene glycol) dimethyl ether (TG) and $LiCF_3SO_3$ salt. The salt was added to give an O:Li ratio (oxygen atoms

* Corresponding author. Fax: +886−2−27376544. E-mail: poda@mail.ntust.edu.tw.

10.1021/ma025831z CCC: $25.00 © 2003 American Chemical Society
Published on Web 08/23/2003

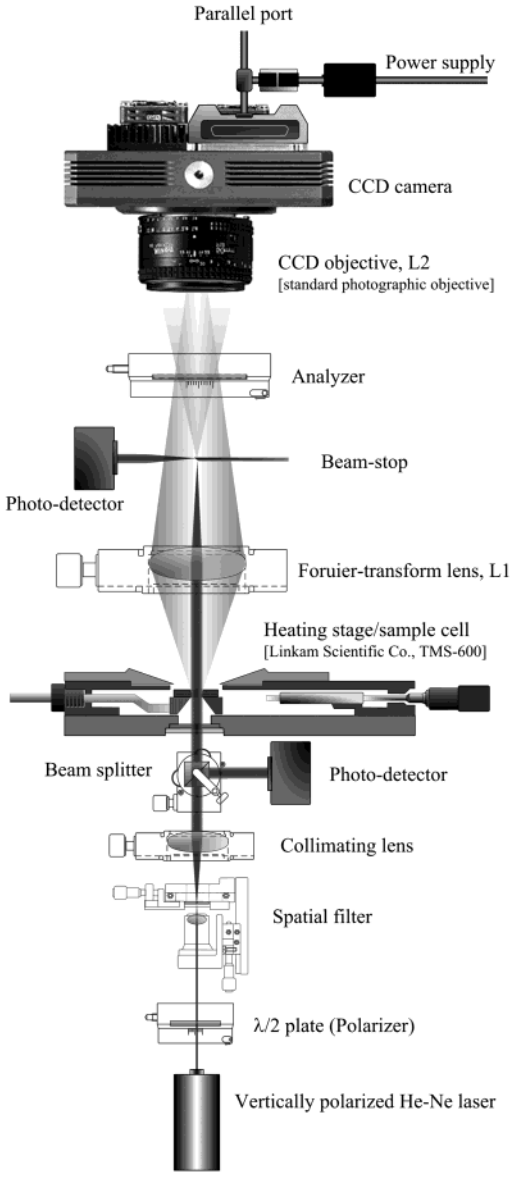

Figure 1. Schematic diagram of the time-resolved small-angle light scattering apparatus. The CCD objective L_2 (a standard photographic objective, Nikon, 50 mm, *f*/1.2) images the focal plane of the collecting lens L_1 onto the CCD sensor with a magnification ratio. Using this optical scheme, a one-to-one mapping between scattering angles and pixel positions on the CCD sensor is realized. A beam stop, made of a 2 mm micro 45° rod mirrors, is placed in the focal plane of the collecting lens L_1 and deviates the transmitted beam by 90° onto a photodetector. The experiments are performed in two geometries: (i) The polarizer and analyzer both have their polarization directions vertical (polarized condition, V_v). (ii) The polarizer and analyzer axes are crossed at 90°, with one polarization direction horizontal and the other vertical (depolarized condition, H_v).

in the TG: Lithium atoms in the salt) of 12:1. The polymer gel electrolytes were prepared by quenching 6 g dL^{-1} homogeneous PVDF solution from 433 K to the gelation temperatures.

TRSALS Measurements. The kinetics of structural evolution was monitored by TRSALS using an experimental setup as sketched in Figure 1. The optical scheme for the collection of the scattered light is similar to that described by Ferri.[20] A plane-polarized laser beam (5 mW He−Ne laser having a wavelength of 632.8 nm) was used as the incident source, and the polarization direction of the beam was varied by a polarization rotator containing a half-wave plate as its essential part. The sample cell was placed on a TMS-600 heating stage (Linkam Scientific Co.) and the scattered light intensity of the sample was directly imaged through a Fourier lens and an analyzer onto the CCD camera (Apogee Instruments Inc., AP 7p with a 512 × 512 pixel sensor) connected to the dynamic image analyzer. The digitized images were acquired by a parallel port interface, which then transferred the real-time processing to a personal computer. In our design the angular range for which reliable data can be collected is about $\theta = 2-25°$, corresponding to $0.497 < q\ (\mu m^{-1}) < 6.159$ [$q = (4\pi n/\lambda) \sin(\theta/2)$, where q is the scattering vector, θ is the scattering angle, n is the refractive index of the medium, and λ is the wavelength of incident light].

Results and Discussion

Figure 2 shows a unique feature of the H_v (depolarized condition) and the V_v (polarized condition) scattering patterns for PVDF gel electrolytes. The results were quite startling in that the H_v scattering pattern could be divided into (i) an X-type scattering pattern with a monotonic decay of the scattering intensity, which at the center of the pattern appears the same as the scattering by an anisotropic rod texture,[21] and (ii) a pattern in the two diagonal directions that appears to have a 4-fold symmetrical pattern at high scattering angles with the maximum scattering intensity. To our knowledge, this complicated H_v scattering pattern has not been observed in physical gel systems. However, a similar scattering pattern has been observed by Nakai et al. in the case of a phase-separated structure formed in polymer blends containing a thermotropic liquid crystalline copolyester as one component.[22,23] Both theoretical analysis and experiments by Nakai et al. indicated that the feature of the 4-fold symmetrical pattern at high scattering angles arises from the coupling of orientation and concentration order parameters. However, we would like to particularly emphasize that there are material and structural differences between the gels and the polymer blends. In addition, we must draw attention to the V_v scattering pattern in our results. In contrast to the V_v scattering in the polymer/liquid crystalline polymer blends, which leads to a pattern with a two-crescent-moon shape along the equator, we obtained only a monotonic decay of the scattering intensity with θ and without azimuthal angle, φ, dependence in the pattern.

On the basis of the Rayleigh−Gans−Debye (RGD) light scattering approximation, Stein and Rhodes gave theoretical expressions for V_v and H_v scattering patterns,[24] referred to as the SR theory. These expressions indicate that the H_v scattering pattern is attributed to optical anisotropic fluctuations (birefringence), whereas the V_v scattering pattern is attributed to both density (refractive index) and optical anisotropic fluctuations. In the case of an anisotropic system, e.g., polymer spherulites, typically calculated scattering patterns predict the four-leaf-clover type pattern for H_v scattering and the two-vertical-lobes type pattern for V_v scattering. Moreover, the SR theory also predicts that intensity of the H_v scattering for isotropic spheres is zero. Although the SR theory is now widely accepted, the above expressions could still not provide a complete explanation for why the V_v scattering has no azimuthal angle dependence, but the H_v scattering reveals a complicated pattern, as shown in Figure 2.

Meeten has confirmed that the four-leaf-clover H_v scattering pattern was also produced by isotropic (amorphous) spheres.[25] On the basis of this fact, the SR theory is incorrect in its prediction that $I_{H_v}(\theta,\varphi) = 0$ for the scattering by isotropic spheres. The reason for this is

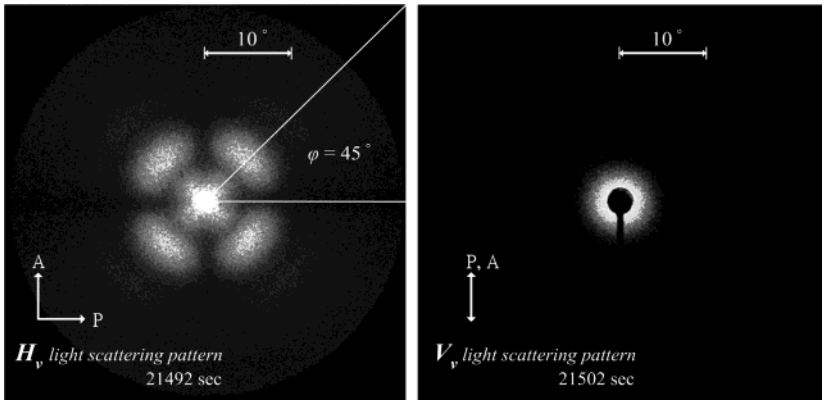

Figure 2. Small-angle light scattering patterns taken under H_v (left) and V_v (right) conditions from a PVDF-TG-$LiCF_3SO_3$ (6 g dL^{-1}) gel at 303 K. The directions of the polarizer and analyzer are shown by arrows.

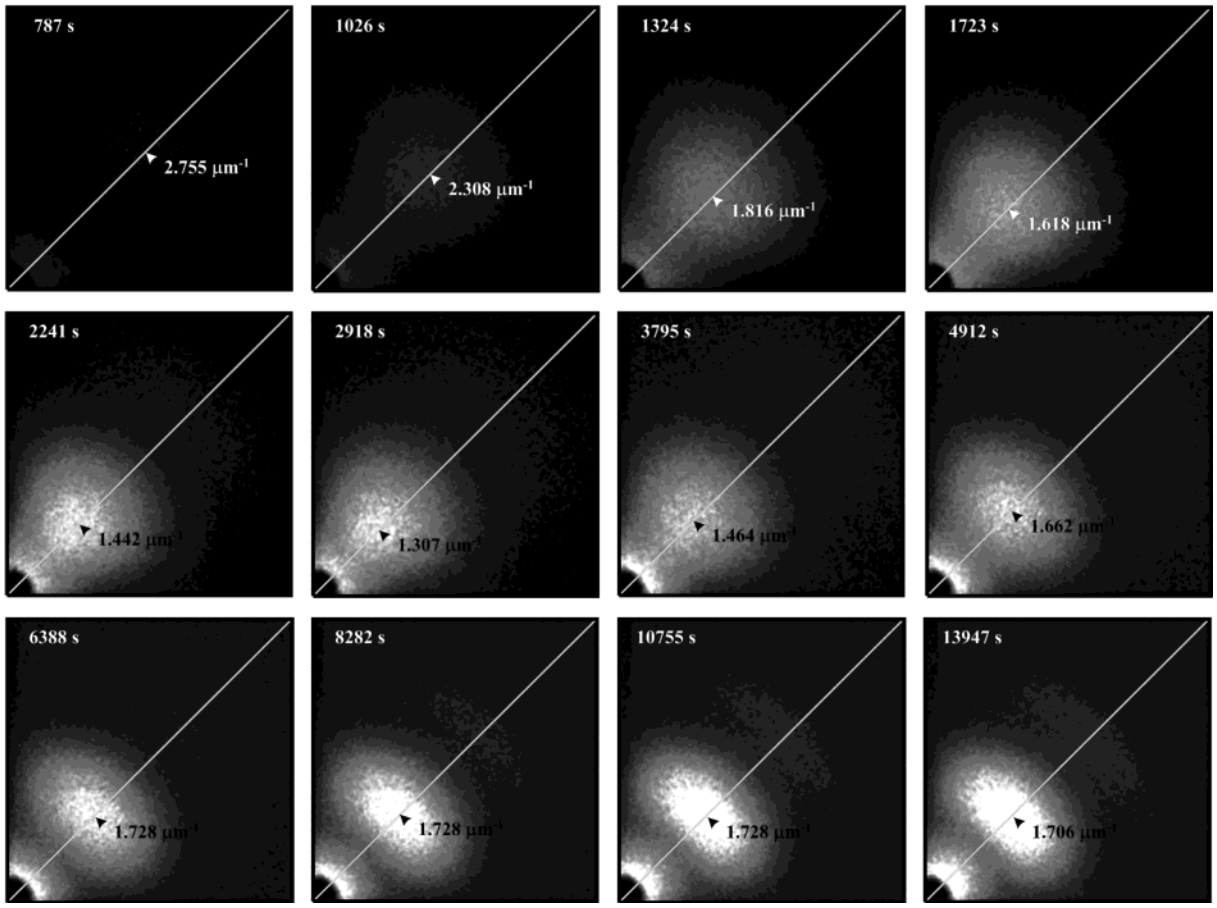

Figure 3. Time evolution of H_v scattering patterns (a quarter pattern) showing the isothermal gelation for 6 g dL^{-1} solution at 303 K. The arrows shown indicate the positions of the scattering vector at which scattering intensity has a maximum value.

considered to be the confusion between the optical properties of the scatterer and the analyzer in the SR theory. Meeten[26] has also given a new expression for light scattering by spherulites and amorphous spheres using the notion and method of van de Hulst.[27] This method first decouples the optical properties of any scatterer from the analyzer and then derives the scattering matrix of any scatterer, which completely describes its scattering properties. It then calculates I_{V_v} and I_{H_v} from the scattering matrix for the given experimental configuration (polarizer, analyzer, and any other components). The more recent expression of Meeten shows in full detail why the four-leaf-clover H_v scattering pattern, previously thought to indicate an optically anisotropic scatterer, is also produced by isotropic spheres. In terms of the scattering intensity without azimuthal angle dependence in our V_v scattering pattern, it seems reasonable to suppose that the origins of the scattering patterns in Figure 2 are produced by aggregation of isotropic spheres. However, Voice et al.[28] have given evidence that the PVDF gel electrolytes contain crystalline components, which act as the major junctions in the gel networks. Thus, there is room for argument on these points, and below we propose a more precise account of these problems.

Having made these distinctions, we should observe that the H_v scattering patterns evolved by the isothermal gelation lead us to further consider the origins of these patterns. A series of H_v scattering patterns are shown in Figure 3. (Note: Because of the biaxial

symmetry of the scattering pattern, we only show the upper-right-quarter pattern.) The arrows indicate the position of the scattering vector when the scattering intensity has a maximum value. It is noteworthy that the time changes in present patterns are not monotonic. The first point to notice is that the growth mode of the characteristic wave vector clearly reveals the existence of three distinct time regimes. Even more significant is the fact that the initial scattering pattern with a four-leaf-clover shape gradually turns into a final pattern with 2-fold structure, which includes an X-type and a four-crescent-moon shape at low and high q range, respectively. The series of H_v scattering patterns as shown above provides a starting point for us to consider the physical gelation process for crystalline polymers in a new light. Before discussing it in detail, we should emphasize that both SR theory and the Meeten expression give a treatment of scattering function for a simply structural model. However, from the universal point of view, the Meeten expression may provide a probable answer to the question in the present work of the underlying origins of the scattering pattern formation by physical gelation. In the case of H_v scattering, the Meeten expression not only is in good agreement with the prediction by SR theory for anisotropic spherulites but also successfully gives a theoretical basis for scattering by isotropic spheres.

The question of what are the patterning differences between the isotropic spheres and the anisotropic spherulites is in H_v scattering has yet to be addressed. In the case of scattering by isotropic spheres, Meeten predicts that the H_v scattering pattern would show a well-defined first-order intensity maximum with the four-leaf-clover shape at low angles, superimposed on many less well-defined higher-order peaks with the four-crescent-moon shape extending to much higher angles.[26] This complicated and interesting pattern was initially experimentally confirmed for a polystyrene latex solution.[29] For the anisotropic spherulites, Meeten predicts that the H_v scattering pattern is generally characterized by the four-leaf-clover pattern, identical to what would be predicted by SR theory. Subsequently, Peuvrel et al. developed this idea further.[30] On the basis of the Meeten expression, adding birefringence to an isotropic sphere to make an anisotropic spherulite is an interesting case, referred to as the isotropic-to-anisotropic transition. The theoretical calculations for this show how the spherical birefringence affects the H_v scattering function in RGD approximation. In the case of positively birefringent spheres, when the spherulitic birefringence is decreased, the characteristics of the H_v structure factor were very similar to our observations shown in Figure 3. Given that the birefingent transition is the core of all the questions regarding the unusual gelation process in this work, we can explain why the unique and complicated scattering patterns are shown in Figure 3. As we noted, the initial scattering patterns with a four-leaf-clover shape implies the growth of the anisotropy spheres, or it may be more accurate to say, the growth of the anisotropy droplets. As time elapses ($t > 2918$ s), the reverse growth of the peak position, conversion of scattering pattern from a four-leaf-clover to a four-crescent-moon shape, and emergence of new first-order peak are the main characteristics of the anisotropic-to-isotropic transition. Having firmly established this point, the next step is to discuss the underlying origins of the anisotropic-to-isotropic transition during the gelation process. However, before we come to that, we should look briefly at the time evolution of light scattering profiles. (Note: We focus only on the H_v scattering in next section, which affords more useful information about the structural formation of the crystalline polymer gels.)

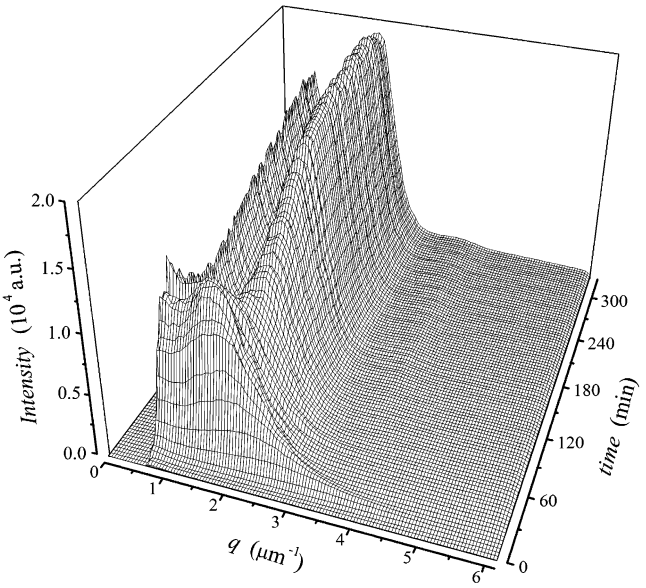

Figure 4. Time evolution of H_v scattering profile at azimuthal angle = 45° for a 6 g dL^{-1} solution after a temperature jump from 433 to 303 K.

Time-resolved scattering profiles obtained for H_v intensity at $\varphi = 45°$ are shown in Figure 4. The first point to notice is that if the time variations of the H_v scattering intensity $I_{H_v}(q,t)$ at various q values have not changed in a certain period of time, then a significant increase in the intensity can be seen. Qualitatively, this behavior is similar to that observed for a nucleation process. Even more noteworthy is the formation of crystallites or fibril texture simultaneous with the emergence of the anisotropy droplets.[13] It is clear that the results of our experiment are entirely different from the general idea of spinodal gels.[4,5,31−33] In terms of two different types of thermodynamic fluctuations, "spinodal decomposition" and "nucleation and growth", many scholars believe that spinodal phase separation occurs in the early stage of gelation and then network formation takes place by interchain crystallization in the concentrated phase.[31,34] However, the evidence shown in Figure 3 questions the basic assumption of this previous assumption.

In view of this, we now attempt to extend our observations to the idea of the coupling of crystal and concentration order parameters on structural characteristics of physical gels. One may safely assume that the crystal nucleation and growth process itself might trigger the concentration fluctuations via the formation of regions of enhanced concentration to form the anisotropic droplets. It also implies that the spontaneous concentration fluctuations by spinodal decomposition are not a necessary condition for the formation of large-scale heterogeneous gels. On the other hand, we can say that the triggered large-scale concentration fluctuations are, in fact, the key to understanding the unusual process for the anisotropic-to-isotropic transition. In other words, the emergence of large-scale concentration fluctuations would dilute the contribution of anisotropic components to the spherical birefringence, yielding the

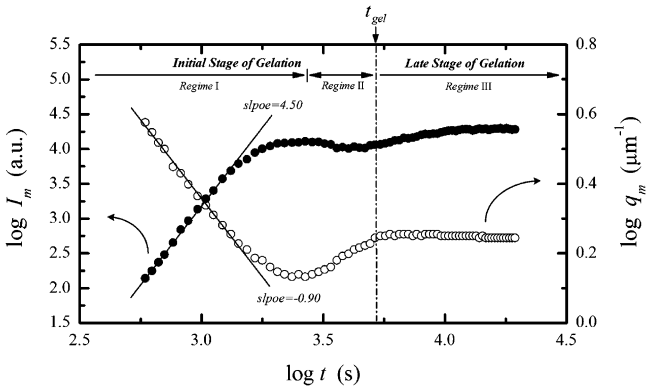

Figure 5. Gelation study. The left abscissa corresponds to the peak intensity I_m (solid circle) while the right one gives the characteristic wave vector q_m (open circle) as a function of the time after a temperature jump.

unique H_v scattering patterns obtained in the present study. We would like to emphasize that this is the first experimental evidence in support of this special birefringent transition. The questions which we must consider next are how to correlate the special birefringent transition with structural formation of the gels and what is a reasonable model for the crystalline polymer gels.

One feature of our results was a marked peak in the scattering intensity distribution at finite q range, with peak intensity gradually rising with time and peak position shifting toward a smaller q range. These facts indicate the growth of the anisotropy droplets, or rather the polymer-rich domain. For each measurement of intensity distribution, we determined the peak intensity I_m as a measure of a characteristic wave vector q_m. The resulting data, as shown in Figure 5, clearly reveal the existence of three distinct time regimes during gelation process. In regime I, there is an initial rapid growth of I_m to a maximum value, accompanied by a decrease in the q_m value. Moreover, both I_m and q_m values exhibit nearly power-law growth behavior in elapsed time ($I_m \sim t^{\beta}$, $q_m \sim t^{-\alpha}$: $\alpha = 0.9$, $\beta = 4.5$). This behavior is qualitatively similar to that observed for spinodal decomposition phenomena; however, this possibility can be excluded, as mentioned earlier. On the other hand, in regime II, we observe a counterintuitive process with a decrease in the I_m value, accompanied by some increase in the q_m value. So far, we have confirmed that this counterintuitive process stemmed from the anisotropic-to-isotropic transition. Following by this intermediate process, there is a moderate growth in the I_m value and cessation of the domain growth during the dynamic process of gelation (regime III). To obtain more detailed information on gelation characteristics, the relationship between the growth of the anisotropic domain and the gelation time is presented in Figure 5. In this study, the test tube tilting method was used to determine the gelation time t_{gel}, which was defined by observing cessation of the liquid flow inside the test tube when it was tilted, and the gelation time was monitored just after the test tube was put into the thermostatic bath. Comparing the scattering result with the gelation time, some distinct features can be seen. The gelation behavior consists of two major stages: (i) an initial stage of gelation from regime I to regime II and (ii) a late stage of gelation in regime III.

To explain this singular gelation behavior, we can discuss the characteristics from the viewpoint of structure factor. In contrast to our system, a wide variety of other systems and processes present the same features in the late stage of the aggregation, growth, or coarsening. Binder has pointed out that the scaled structure factor $S(q,t)$ could be scaled according to a universal law[35,36]

$$S(q,t) = q_m^{-d}(t)\tilde{S}[q\Lambda(t)] \tag{1}$$

where $\Lambda(t)$ is the correlation length corresponding to $q_m(t)^{-1}$; $\tilde{S}[q\Lambda(t)]$ is a time-independent scaling function which depends only on the shape the structures; and d is the dimensionality of the systems, where $d = 3$ for spinodal decomposition or crystal growth, whereas $d = d_f = 1.8$ for diffusion-limited cluster aggregation.[37] Here d_f is the fractal dimension of the cluster. We should notice that this relation holds only if mean-square concentration fluctuations have a time-independent constant value. Thus, the time evolution of the structure factor should be scaled with a single time-dependent length parameter $\Lambda(t)$. Although the data are not shown here, the present structure factor cannot be scaled by any means with a single length parameter due to the mean-square concentration fluctuations, the correlation length, and the birefringence change with time during the isothermal gelation process. Thus, we would like to explore what the global structural evolution is in the gelation process. We felt this process should be reasonably central in the sense that proposes a clear physical picture for the gels formation. For the sake of qualitative discussion, we rescaled our scattering data by

$$\tilde{S}(x) = I(q,t)/I(q_m,t), \quad x = q/q_m(t) \tag{2}$$

where $\tilde{S}(x)$ is the scaled structure factor and x is the reduced wavenumber. To obtain more detailed information on the measured structure factor, the data were fitted by the Furukawa form[38]

$$\tilde{S}(x) \sim \frac{x^2}{\gamma/2 + x^{2+\gamma}} \tag{3}$$

where γ is defined as $\gamma = d + 1$ for the cluster structure and $\gamma = 2d$ for the percolation structure, in which d is the dimensionality of the systems. Figure 6 shows the double logarithmic plot of $\tilde{S}(x)$ vs x in regimes I−III. The theoretical curves for the cluster and percolation structures are also shown in Figure 6 by solid and broken lines, respectively. In regime Ia, the structure factors are universal and an asymptotic behavior of x^{-4} at $x > 1$ indicates the self-similar growth of cluster structures at the large distance scale. On the other hand, $\tilde{S}(x)$ is nonuniversal at larger values of x ($x > 1.5$), as indicated by an arrow in regime Ib, and it exhibits the crossover in its asymptotic behavior with x. Nevertheless, the features of global structure also obey the growth law of droplets (cluster regime). We noted above that regime I exhibits nearly power-law growth behavior in elapsed time. More noteworthy is that the feature of time-evolution of light scattering intensity profilers at an early stage is qualitatively similar to the nucleation process. From what has been said above, regime I can be interpreted in terms of the nucleation of clusters accompanied by some growth. To borrow Schätzel's method,[39] we may reasonably assume a constant nucleation rate and a self-similar growth of the clusters in this early stage. Therefore, the cluster growth may have

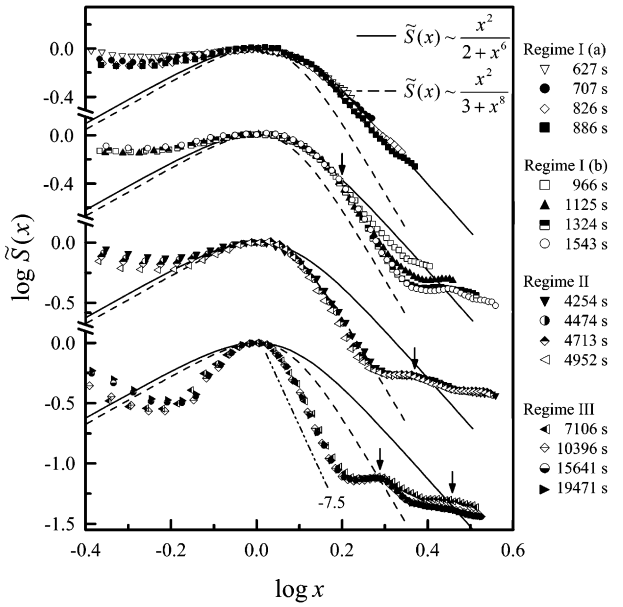

Figure 6. Scaled structure−function in two time regimes, "initial stage of gelation" (regime I and regime II) and "late stage of gelation" (regime III). The solid and broken curves are due to Furukawa's theory.

a scaling law of $q_m \sim t^{-\alpha}$ and $I_m \sim t^{-d\alpha+1} \sim t^{\beta}$. In accordance with this scaling relationship we may expect $\beta = 3.7$ for the three-dimensional cluster growth and $\beta = 2.62$ for the fractal cluster growth. The experimental results show that I_m obeys the power law of $t^{4.5}$ greater than the expected value from the scaling relationship. However, the value is close to the expected one from the growth of three-dimensional clusters, or rather the growth of the "isolated birefringent droplets". We may, therefore, reasonably conclude that no fractal cluster aggregation was observed at least in this stage. For the explanation of this deviation from the growth exponent of three-dimensional clusters, one may point to the growth process of isolated birefringent droplets as the characteristic wavelength, the amplitude of concentration fluctuations, and birefringence increase simultaneously with time. All this may be sufficient to explain why the dynamic scaling hypothesis, expressed by eq 1, is found to break down for the gelation process.

In regime II, a counterintuitive growth process was observed, wherein the process does not conform to the general mechanism of the droplet coarsening, as in the diffusion−reaction process,[35] or the evaporation-condensation process (Lifshitz−Slyozov ripening[40]). At this point the counterintuitive growth process has been considered now that we are sure of the growth process in connection with the special birefringent transition, which is triggered by large-scale concentration fluctuations. The next step is to consider how we could provide a convincing explanation as to the origins of the triggered large-scale concentration fluctuations during the gelation process. The structure factor may give evidence to solve this perplexing problem. As shown in Figure 6, the asymptotic behavior of $\tilde{S}(x)$ at $x > 1[\tilde{S}(x) \sim x^{-n}]$ changes from $n = 4$ to $n = 6$, suggesting that the triggered large-scale concentration fluctuations are due to "*the dynamic crossover of domain growth behavior from cluster to percolation structure*". The inverse process, i.e., a dynamic percolation-to-cluster transition, has been observed experimentally in the spinodal decomposition of an off-critical polymer blend by Takeno and Hashimoto.[41] They suggest that, as the phase separation proceeds and the domain structure grows, the domains rich in minority components are not able to maintain the macroscopic percolation, and then transform into isolated droplets.[42] However, the results of our experiment are contrary to the common cases. One possibility is to assume that the peculiar feature of the cluster-to-percolation transition in regime II can be regarded as a case of hard-sphere colloid aggregation,[14,15,37,43] wherein the cluster diffusion plays an essential role to form a long-range intercluster structural order. In many such cases, it has been shown that the colloidal aggregation exhibits a feature similar to the system undergoing spinodal decomposition. This assumption drives us to the question of whether the isolated birefringent droplets can be regarded as the hard spheres. In the preceding section, we pointed out that cluster formation in regime I can be interpreted in terms of the simultaneous formation of crystallites or fibrils texture with the growth of the birefringent droplets. According to previous reports,[13,28] we may say that the crystallites or fibrils act as junction points for intermolecular cross-linking in the droplets, leading to the formation of the microgels and approximate dispersion of the hard spheres in the solutions. From the point of view of colloid aggregation, it seems reasonable to infer that the triggered large-scale concentration fluctuation is the inevitable result of the isolated droplets diffusion to form the macroscopic percolation structure.[44,45] Therefore, the colloid aggregation dominates the gelation process in this stage.

The novel aspects of the dynamic cluster-to-percolation transition and the accompanied behavior for the special birefringent transition are observed for the first time in the structural evolution during physical gelation. The point we wish to emphasize here is that the spatially bicontinuous percolation structure is one of the main characteristics in physical gelation, and it would be expected that the domain growth behavior is restrained by the macroscopic gelation in regime III. As shown in Figure 5, the gel is formed after the dynamic cluster-to-percolation transition has eventually pinned down domain growth during the intercluster cross-linking. Moreover, a moderate growth in peak intensity indicates a ripening process in late stage gelation, where it causes the arrangement and the growth of microstructure such as crystallites or fibrils texture to be highly concentrated. In Figure 6, we also present a plot of the scaled structure factor $\tilde{S}(x)$ vs x in late stage of gelation. The $\tilde{S}(x)$ has x^{-n} ($n \approx 7.5$) dependence for $1 < x < 1.5$, and this form is in agreement with other experimental results of $\tilde{S}(x)$ for the structural formation of percolation or bicontinuous domain during spinodal decomposition of a polymer blend.[41] Viewed in this light, the sharpening in $\tilde{S}(x)$ can be regarded as a ripening process in a late stage of gelation. It is also worth mentioning that the $\tilde{S}(x)$ in the regime exhibits a shoulder or a second-order maximum at $x \approx 2.4$, as indicated by an arrow. Moreover, in the late stage of gelation, we observed a more complex structure factor that shows at least a third-order maximum at $x > 1.5$, as indicated by an arrow. We tentatively consider that such a phenomenon is related to a local structure, probably consisting of an interface structure or arising from single droplet. However, this subject cannot be discussed in detail here for lack of space, and it will be taken up in our next study.

Conclusion

In this work, we report the first real-time observation of crystal nucleation and concentration fluctuation during the physical gelation process of a crystalline polymer. It is clear that the experimental results are entirely different from the general concept of spinodal gels. It also implies that the spontaneous concentration fluctuation by spinodal decomposition is not a prerequisite for the formation of large-scale heterogeneous gels. In particular, these observations illustrate the novel aspect on the structural formation of the physical gels.

Our results show that the gelation process can be governed by the coupling of several phase transitions. In the initial stage, the mechanism of the birefringent droplet nucleation and growth can be regarded as the coupling of two different type phase transitions, i.e., crystallization and liquid−liquid-phase separation. Viewed in this light, we would question whether the formation of the birefringent droplet can be compared to the nonclassical "spinodal" nucleation.[45] However, there is need for further investigation on this question. In the intermediate stage, the hard-sphere-like colloid aggregation dominates the gelation process. The key idea for aggregation in colloidal suspensions has been demonstrated by its *fractal* nature, and the gelation may be considered as a direct consequence of the growth of *fractal* structures. According to the sticking probability, two limiting regimes of the aggregation process have been identified, namely, diffusion-limited cluster aggregation (DLCA) and reaction-limited cluster aggregation (RLCA). As we have mentioned above, the formation of the spatially bicontinuous percolation structure is a decisive stage for gelation, and it is constructed by the isolated droplet diffusion to form the macroscopic percolation structure i.e., dynamic cluster-to-percolation transition. Thus, the DLCA model clearly appears to be a better model for this case than the RLCA model. However, there is not enough evidence to support the fractal aggregation of the birefringent droplets in the present work. In addition, it might be worth mentioning that Tanaka and Araki developed a new simulation method of colloidal suspensions with hydrodynamic interactions ("fluid particle dynamics" method, FPD).[44] They demonstrated that the hydrodynamic interactions crucially affect the structure evolution and kinetics of aggregation, gel formation, and phase separation in colloidal suspensions. Where there are no hydrodynamic interactions, particles may tend to aggregate into a much more compact structures, the same as reported in Brownian-dynamic-like simulations. With hydrodynamic interactions, simulated by FPD method, the flow fields induced by the motion of a particle pair significantly increase the probability of the formation of a chainlike open structure (percolation structure). As Tanaka and Araki pointed out, the hydrodynamic interactions between particles are quite important to an understanding of the formation of a transient gel of colloidal particles. Of course, having suggested that the dynamic cluster-to-percolation transition is due to interdroplet hydrodynamic interactions, we still have a long way to go before obtaining evidence to support this proposal.

Acknowledgment. The authors would like to thank the National Science Council of the Republic of China for financially supporting this research under Contract No. NSC-90-2216-E-011-029.

References and Notes

(1) Stauffer, D.; Coniglio, A.; Adam, M. *Adv. Polym. Sci.* **1982**, *44*, 105.
(2) Coniglio, A.; Stanley, H. E.; Klein, W. *Phys. Rev. Lett.* **1977**, *42*, 518.
(3) Keller, A. *Faraday Discuss. Chem. Soc.* **1995**, *110*, 1.
(4) Tanaka, T.; Swislow, G.; Ohmine, I. *Phys. Rev. Lett.* **1979**, *42*, 1556.
(5) Asnghi, D.; Giglio, M.; Bossi, A.; Righetti, P. G. *J. Chem. Phys.* **1995**, *102*, 9736.
(6) Tanigami, T.; Suzuki, H.; Yamaura, K.; Matsuzawa, S. *Macromolecules* **1985**, *18*, 2595.
(7) Godard, J.; Biebuyck, J. J.; Dumerie, M.; Naveau, H.; Mercier, J. P. *J. Polym. Sci., Part B: Polym. Phys.* **1978**, *16*, 1817.
(8) Stepto, R. F. T. *Polymer Networks Principles of their Formation, Structure and Properties*; Blackie Academic & Professional: London, 1998.
(9) Burchard, W.; Ross-Murphy, S. B. *Physical Networks Polymer and Gels*; Elsevier: London, 1998.
(10) te Nijenhuis, K. *Thermoreversible Networks*; Springer: New York, 1997.
(11) Guenet, J. M. *Thermoreversible Gelation of Polymers and Biopolymers*; Academic Press: London, 1992.
(12) Hong, P. D.; Chou, C. M. *Macromolecules* **2000**, *33*, 9673.
(13) Hong, P. D.; Chou, C. M. *Polymer* **2000**, *41*, 8311.
(14) Schätzel, K.; Ackerson, B. J. *Phys. Rev. Lett.* **1992**, *68*, 337.
(15) Carpineti, M.; Giglio, M. *Phys. Rev. Lett.* **1992**, *68*, 3327.
(16) Takenaka, M.; Izumitani, T.; Hashimoto, T. *J. Chem. Phys.* **1990**, *92*, 4566.
(17) Bates, F. S.; Wiltzius, P. *J. Chem. Phys.* **1989**, *91*, 3258.
(18) Monno, M.; Palma, M. U. *Phys. Rev. Lett.* **1997**, *79*, 4286.
(19) Takeshita, H.; Kanaya, T.; Nishidam, K.; Kaji, K. *Macromolecules* **1999**, *32*, 7815.
(20) Ferri, F. *Rev. Sci. Instrum.* **1997**, *68*, 2265.
(21) Rhodes, M. B.; Stein, R. S. *J. Polym. Sci., Part A-2* **1996**, *7*, 1539.
(22) Nakia, A.; Shiwaku, T.; Hasegawa, H.; Hashimoto, T. *Macromolecules* **1986**, *19*, 3008.
(23) Nakia, A.; Shiwaku, T.; Wang, W.; Hasegawa, H.; Hashimoto, T. *Polymer* **1996**, *37*, 2259.
(24) Stein, R. S.; Rhodes, M. B. *J. Appl. Phys.* **1960**, *31*, 1873.
(25) Meeten, G. H. *J. Polym. Sci., Part B: Polym. Phys.* **1984**, *22*, 2159.
(26) Meeten, G. H. *J. Polym. Sci., Part B: Polym. Phys.* **1989**, *27*, 2023.
(27) Van de Hulst, H. C. *Light Scattering by Small Particles*; John Wiley & Sons: New York, 1957.
(28) Voice, A. M.; Southall, J. P.; Rogers, V.; Matthews, K. H.; Davies, G. R.; Mclntyre, J. E.; Ward, I. M. *Polymer* **1994**, *35*, 3363.
(29) Desbrodes, M.; Meeten, G. H.; Navard, P. *J. Polym. Sci., Part B: Polym. Phys.* **1989**, *27*, 2037.
(30) Peuvrel, E.; Siegert, D.; Navard, P.; Meeten, G. H. *J. Polym. Sci., Part B: Polym. Phys.* **1992**, *30*, 865.
(31) Tromp, R. H.; Rennie, A. R.; Jones, R. A. L. *Macromolecules* **1995**, *28*, 4129.
(32) Takeshita, H.; Kanaya, T.; Nishida, K.; Kaji, K. *Macromolecules* **1999**, *32*, 7815.
(33) Loren, N.; Altskar, A.; Hermansson, A. M. *Macromolecules* **2001**, *34*, 8117.
(34) Ransil, R.; Lal, J.; Carvalho, B. L. *Polymer* **1992**, *33*, 2961.
(35) Binder, K.; Stauffer, D. *Phys. Rev. Lett.* **1974**, *33*, 1006.
(36) Binder, K. *Phys. Rev. B* **1977**, *15*, 4425.
(37) González, A. E.; Santiago, G. R. *Phys. Rev. Lett.* **1995**, *74*, 1238.
(38) Furukawa, H. *Adv. Phys.* **1985**, *34*, 703.
(39) Schätzel, K.; Ackerson, B. J. *Phys. Rev. E* **1993**, *48*, 3766.
(40) Lifshitz, I. M.; Slyozov, V. V. *J. Phys. Chem. Solids* **1961**, *19*, 35.
(41) Takeno, H.; Hashimoto, T. *J. Chem. Phys.* **1997**, *107*, 1634.
(42) Hashimoto, T.; Takenaka, M.; Izumitani, T. *J. Chem. Phys.* **1992**, *97*, 679.
(43) Carpineti, M.; Giglio, M. *Phys. Rev. Lett.* **1992**, *68*, 3327.
(44) Tanaka, H.; Araki, T. *Phys. Rev. Lett.* **2000**, *85*, 1338.
(45) Poon, W. C. K.; Haw, M. D. *Adv. Colloid Interface Sci.* **1997**, *73*, 71.

MA025831Z